Multiple-Pulse Nuclear Magnetic Resonance of Solid Polymers. Polymer Motions in Crystalline and Amorphous Poly(tetrafluoroethylene)†

A. J. Vega and A. D. English*

Central Research and Development Department, E. I. du Pont de Nemours and Company, Experimental Station, Wilmington, Delaware 19898. *Received December 12, 1979*

ABSTRACT: ^{19}F NMR chemical shift spectra obtained with a multiple-pulse sequence are shown to be useful in determining crystallinity and detecting macromolecular motion in randomly oriented poly(tetrafluoroethylene) and poly(tetrafluoroethylene–hexafluoropropylene). The β relaxation in PTFE is observed and our results are in agreement with previous anelastic and dielectric measurements. The γ relaxation is observed and is shown to be due to reorientation about a local chain axis in the amorphous regions. Chain-axis reorientation in the amorphous regions, which has not been observed in previous measurements, is observed to be very rapid ($\gtrsim$100 MHz) and to grow in amplitude with increasing temperature. The TFE/HFP copolymer exhibits the same types of macromolecular motions, but the amorphous-region local chain axis reorientation is inhibited by the sterically larger CF_3 groups below the melting point.

Introduction

Previous studies of poly(tetrafluoroethylene) (PTFE) by conventional[1-5] and multiple-pulse NMR[6-8] have given considerable insight into the different types of polymer motion that are present in both crystalline and amorphous regions. We have reported[9] preliminary results of the use of multiple-pulse NMR to examine polymer crystallinity and motion in PTFE. We report here an extensive study of randomly oriented PTFE (melt recrystallized and virgin), PTFE fibers, and a randomly oriented copolymer of tetrafluoroethylene and hexafluoropropylene.

Multiple-pulse NMR is used for two reasons: one, to determine what new information multiple-pulse NMR could make available that is not available for polymeric solids from conventional NMR (broad line and relaxation studies (T_1,T_2,$T_{1\rho}$)), and two, to determine for PTFE what types of macromolecular motions are detectable in both the crystalline and the *amorphous* phases. Previous conventional NMR studies of PTFE have been summarized;[4] however, a brief synopsis will be useful in contrasting the types of information available from conventional and multiple-pulse NMR. Conventional NMR experiments on PTFE have been useful in determining approximate values for the crystallinity, observing the first-order crystalline-phase transition at 19 °C, confirming that the crystalline-phase transition involves reorientation about the chain axis,[3] and measuring various relaxation times (T_1,T_2,$T_{1\rho}$), some of which can be correlated[4] with previously known relaxations. Conventional NMR results were not able to independently relate a specific relaxation process with a specific macromolecular motion in randomly oriented samples. A study of oriented fibers[3,39] has confirmed that the 19 °C crystalline transition involves reorientation about the chain axis.

Previous multiple-pulse NMR studies have determined that ^{19}F chemical shift spectra of fluoro polymers can be obtained,[6] that the principal values of the chemical shift tensor can be determined in a randomly oriented sample,[8] and, additionally, that the orientation of the chemical shift tensor with respect to a molecular axis system can be determined for an oriented sample.[7] However, these previous studies did not address themselves to the use of multiple-pulse NMR to determine crystallinity or to observe various motions and/or relaxations. More recently,[1]H multiple-pulse studies have been used to determine a value for the crystallinity of a polyethylene sample[10] that was in reasonable agreement with a value determined calorimetrically. We have shown[9] that ^{19}F chemical shift spectra obtained with multiple-pulse techniques can be used to determine crystallinity and to directly observe general types of macromolecular motions in polycrystalline PTFE. Our present results demonstrate that chemical shift spectra obtained with multiple-pulse techniques can be used to obtain well-defined values of polymer crystallinity that correlate well with other measurements and, when combined with relaxation measurements, can be used to *directly detect macromolecular motions in both crystalline and amorphous regions in randomly oriented samples.*

Multiple-pulse NMR techniques are a powerful tool for studying polymers and other solids because the NMR spectra obtained are dominated by chemical shift rather than dipolar interactions. The use of isotropic chemical shift spectra to study molecules in solution has been known as a powerful tool for the study of structure and chemical-exchange mechanisms for at least 20 years.[11] Chemical shift spectra are not usually observed for solids because the chemical shift interaction is overwhelmed and obscured by the nuclear dipolar interactions. Conventional NMR spectra, dominated by dipolar interactions, are usually very broad and rather featureless in all but the simplest systems and are usually characterized by only a single variable, the second moment. The dipolar spectrum is featureless because the dipolar term in the nuclear spin Hamiltonian is a many-spin operator which represents the interactions of any one spin with all other spins in the sample. (Although we often only need to concern ouselves with those spins within $\lesssim$20-Å radius, there are still 10–100 interactions that are important.) Conversely, the chemical shift interaction is a single spin operator, and a chemical shift powder pattern is characterized by two values of the chemical shift tensor. More importantly, the structure in the chemical shift pattern is a quite sensitive probe of not only the rate but also the type of motion taking place in the sample. This last feature of chemical shift spectra is the main reason for their use in polymer NMR.

Experimental Section

The spectrometer used was a Bruker SXP-100 NMR spectrometer slightly modified for high-temperature[14] multiple-pulse operation. The unmodified commercial spectrometer is capable of only the simplest multiple-pulse experiments; however, careful matching of the probe circuit as a function of temperature allows

† Contribution No. 2719.

0024-9297/80/2213-1635$01.00/0

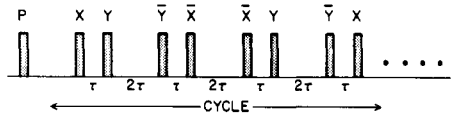

Figure 1. REV-8 multiple-pulse sequence used in these experiments. The sequence consists of a string of identical cycles of eight 90° radio-frequency pulses with relative phases as indicated. The sequence is preceded by a preparatory 90° pulse (P). For line-shape measurements the phase of P is alternately x or $-x$; for T_{1xz}^{REV} measurements P is alternately absent or $-y$ (see text). The NMR signal is sampled at the end of each cycle. $\tau = 3.6$ μs.

multiple-pulse spectra to be routinely obtained.

The NMR spectra were acquired by using the REV-8 sequence,[15] which consists of a long train of closely spaced, high-power radio-frequency pulses of fixed width, varying in phase in a cyclical fashion. The cycle (Figure 1) consists of eight $\pi/2$ pulses. The total cycle time used was 43.2 μs with a shortest spacing between pulses of 3.6 μs. The nominal resonance frequency was 84.6 MHz, a $\pi/2$ pulse was 2.2 μs, and the data were acquired with the carrier frequency below resonance (the right-hand side of the spectrum in each figure). It is convenient to tune the spectrometer following the procedure given by Rhim et al.[16] We estimated that the radio-frequency inhomogeneity was 0.5–1.0%. The spectrometer tuning must be checked and readjusted if the temperature is changed by more than ±30 °C. The chemical shift scaling factor was experimentally measured each time the spectrometer was retuned by determining the resonance positions of a liquid sample taken off resonance in steps of 2 kHz up to 16 kHz. The resulting frequency dependence was not linear but could be fitted to a quadratic relationship which was used in the line-shape analysis.

The data were acquired by sampling the signal once per cycle until approximately 500 points were acquired (20-ms pulse train). These data are unsatisfactory for Fourier transformation because of large base-line shifts and nonlinear base lines. This problem is avoided by adding and subtracting in the computer memory the data obtained from two n pulse trains, where n pulse trains are preceded by an x prepulse and the other n pulse trains by a $-x$ prepulse (see Figure 1), so that the observed signal is either positive or negative in phase. This procedure produces data that, when Fourier transformed, are essentially free of base-line artifacts and spurious signals. The total accumulation time for one spectrum was less than 10 min.

Spin–lattice relaxation times in the multiple-pulse interaction frame were measured by using the same eight pulse cycle but with different prepulses.[13] Here the prepulse is alternatively absent or $-y$ so that the net result of the add/subtract procedure is to cancel out all signals except that part which is effectively spin locked in the (101) direction in the interaction frame. This relaxation time (T_{1xz}^{REV}) is determined by measuring the amplitude of the spin-locked signal stroboscopically during the multiple-pulse irradiation.

The polymer samples were contained in 5-mm NMR tubes and all were unoriented except for PTFE fibers. The samples included virgin (granular and aqueous dispersion) PTFE, melt-recrystallized PTFE, annealed virgin PTFE, PTFE fibers, and a copolymer of tetrafluoroethylene and hexafluoropropylene.

Annealed virgin samples were prepared by heating virgin PTFE samples to slightly below the virgin melting point (347 °C) and then cooling, in an attempt to prepare highly crystalline samples similar in morphology to melt-recrystallized samples. Melt-recrystallized samples of varying crystallinity were prepared by varying the rate of cooling of melted PTFE. Virgin PTFE and PTFE fibers were commercially available samples (Du Pont).

Results

Variable-temperature (−150 to +350 °C) chemical shift spectra have been obtained for melt-recrystallized, annealed virgin, virgin, and fiber samples of PTFE and for a copolymer of TFE and HFP. These spectra may be used to determine polymer crystallinity and to determine various kinds of macromolecular motion. Also spin–lattice relaxation times in the radio-frequency interaction frame (T_{1xz}^{REV}) in addition to conventional T_1 and $T_{1\rho}$ relaxation

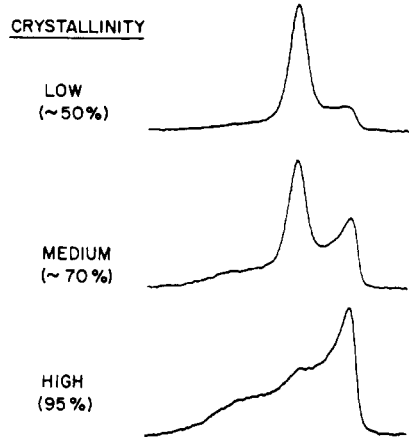

Figure 2. ^{19}F REV-8 chemical shift spectra of PTFE samples of varying crystallinity obtained at 259 °C. The total width of the spectra is about 17 kHz.

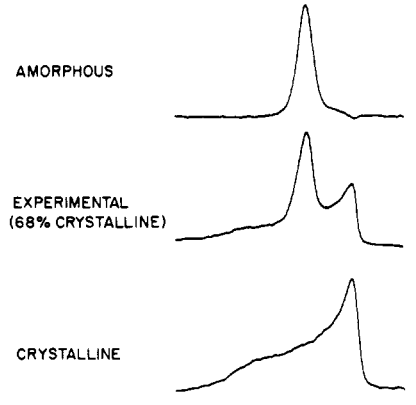

Figure 3. ^{19}F REV-8 chemical shift line shapes of a 68% crystalline PTFE sample at 259 °C and decomposed line shapes of the amorphous and crystalline fractions.

times have been measured to help elucidate the various mechanisms responsible for the observed chemical shift line shapes.

With a few exceptions, the results of all randomly oriented PTFE samples follow a general dependence on temperature and degree of crystallinity. These general results will be discussed first. Unusual behavior is observed in the virgin and annealed virgin PTFE samples. The results obtained for the fibers and the TFE/HFP copolymer are presented separately.

General Observations. Chemical shift spectra of PTFE obtained at 259 °C are shown in Figure 2. These line shapes, for three different samples of varying crystallinity, may be seen to be a linear combination of two line shapes: one is characteristic of an axially symmetric powder pattern and the other of an isotropic chemical shift tensor. At this temperature these two line shapes differ greatly and they are easily decomposed by a numerical method (see Appendix A).

In Figure 3, these line shapes are decomposed into the isotropic line shape and the axially symmetric powder pattern line shape. This same procedure was used for eight samples of melt-recrystallized and annealed virgin PTFE. As discussed in Appendix A, this decomposition procedure shows that the spectra consist almost exclusively of only two fractions, with the narrow component obviously corresponding to the amorphous fraction of the polymer and the axially symmetric powder pattern to the crystalline fraction. Moreover, the amorphous as well as the crystalline line shapes extracted from samples of different crystallinity are essentially identical, which indicates that

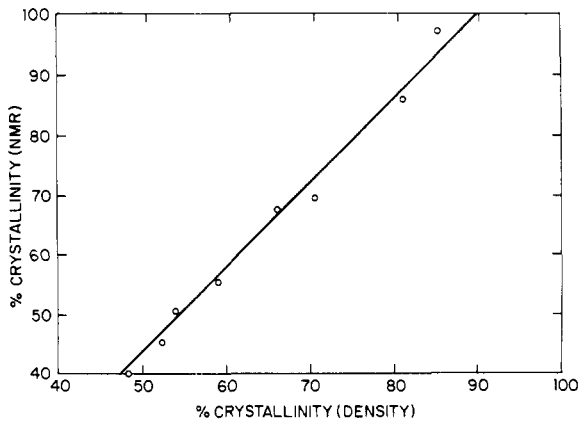

Figure 4. Crystallinities of several melt-processed and annealed virgin PTFE samples as determined from decomposition of chemical shift line shapes vs. crystallinities determined from density measurements.

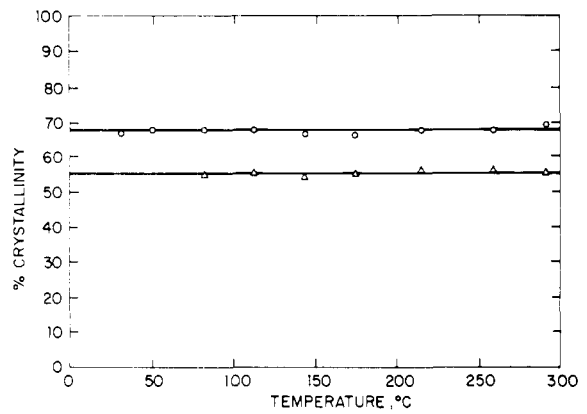

Figure 5. Temperature dependence of the crystallinities of two melt-processed PTFE samples as determined from decomposition of chemical shift line shapes.

the structure and dynamics in the crystalline and amorphous fractions are independent of the degree of crystallinity.

The relative contributions to the intensity of a composite line shape are thus a measure of the degree of crystallinity of the PTFE sample. The crystallinities determined in this fashion are compared to values determined by density[17,18] measurements in Figure 4. These results indicate an excellent correlation between crystallinities measured with the two techniques; however, the agreement is not absolute, which is not unusual when comparing values of crystallinity measured by different techniques which use different criteria for crystallinity.[19] We also determined the crystallinity of as-polymerized, both granular and aqueous dispersion, PTFE to be 99.7%. In addition, the crystallinity can be determined as a function of temperature by the same line-shape decomposition process. These results (Figure 5) indicate that this method of crystallinity determination is independent of temperature for PTFE above 30 °C within ±3% and is probably superior to X-ray or infrared methods in this regard.[17-19]

Decomposed chemical shift spectra of melt-recrystallized PTFE at three temperatures (Figure 6) illustrate that both the crystalline and amorphous regions of the polymer undergo extensive line-shape changes over this temperature range. The amorphous line shape (left side of Figure 6) is completely asymmetric at the lowest temperature but at sufficiently high temperatures becomes symmetric; the crystalline line shape is also asymmetric at the lowest temperature but retains axial symmetry to at least 259 °C. In fact, the crystalline line shape remains axially symmetric

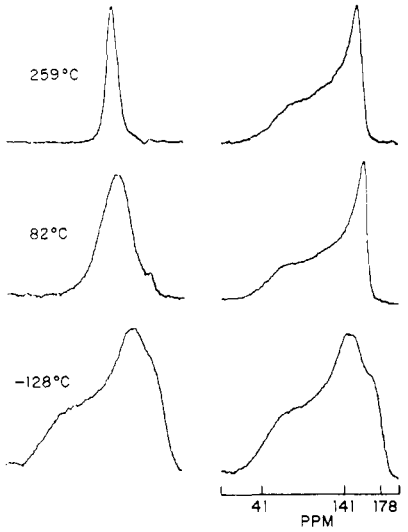

Figure 6. Decomposed ^{19}F REV-8 chemical shift spectra of the amorphous (left) and crystalline (right) fractions of PTFE at various temperatures.

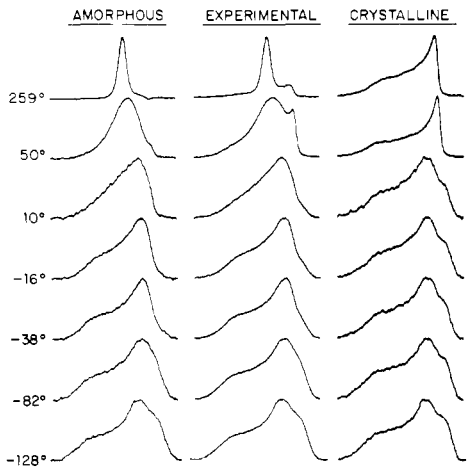

Figure 7. ^{19}F REV-8 chemical shift line shapes of melt-recrystallized PTFE at various temperatures. The experimental spectra (center) are of a 68% crystalline sample. The amorphous (left) and crystalline (right) line shapes were obtained by decomposition of experimental spectra.

to very near the melting point (327 °C). Additionally, the crystalline and amorphous line shapes have very nearly the same line shape at the lowest temperature (the line shapes are invariant to temperature below −128 °C), indicating that in the slow-motion limit the environments of the amorphous and crystalline regions are essentially indistinguishable with these techniques. The figure also gives the three principal components of the chemical shift tensor as σ_{xx} = 178 ppm, σ_{yy} = 141 ppm, σ_{zz} = 41 ppm with respect to $CFCl_3$ (see Appendix B).

A more complete set of decomposed line shapes (Figure 7) allows us to make more detailed conclusions about the macromolecular motions in the crystalline and amorphous regions. The crystalline line shape is seen to retain the asymmetric line shape until ~10 °C and to reach a completely axially symmetric line shape by ~30 °C. The crystalline line shapes are amenable to a detailed study of the rate at which the line shape changes from asymmetric to axially symmetric. Figure 8 shows small temperature increments during which the crystalline line shape undergoes this transformation. The temperature dependence of these line shapes can be simulated by a model of rotational diffusion about the chain axis and these calculated spectra are also shown in Figure 8. (See Ap-

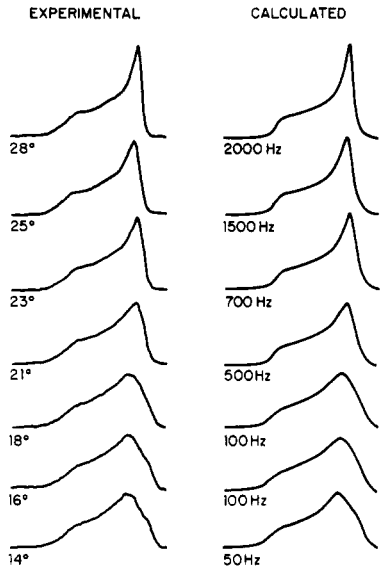

Figure 8. Experimental ^{19}F REV-8 chemical shift line shapes of the crystalline fraction of melt-recrystallized PTFE between 14 and 28 °C (left) and calculated line shapes for rotational diffusion about the chain axis with diffusion coefficient as indicated (right).

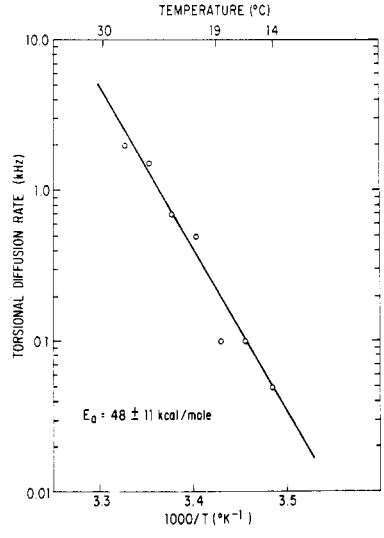

Figure 9. Temperature dependence of the rate of rotational diffusion about the chain axis of PTFE molecules in the crystalline regions of melt-recrystallized samples.

pendix C for details of the calculations.) The temperature dependence of the rate of this process is shown as an Arrhenius plot in Figure 9 and the calculated least-squares-fitted activation energy is 48 ± 11 kcal/mol (95% confidence limits).

The amorphous line shape becomes axially symmetric by −60 °C and then begins to collapse into a symmetric line shape. The transformation of the amorphous line shape from asymmetric to axially symmetric is imprecisely defined because the process which transforms it into a symmetric line shape becomes dominant before the line shape becomes completely axially symmetric. Figure 10 shows in detail representative amorphous chemical shift line shapes as a function of temperature.

In addition to chemical shift spectra, T_1, $T_{1\rho}$, and T_{1xz}^{REV} were measured for many of the samples as a function of temperature. The T_1 results agreed well with those previously obtained by McCall et al.[4] Figure 11 gives values of $T_{1\rho}$ and T_{1xz}^{REV} for one of the melt-recrystallized samples as a function of temperature. Both the $T_{1\rho}$ and T_{1xz}^{REV}

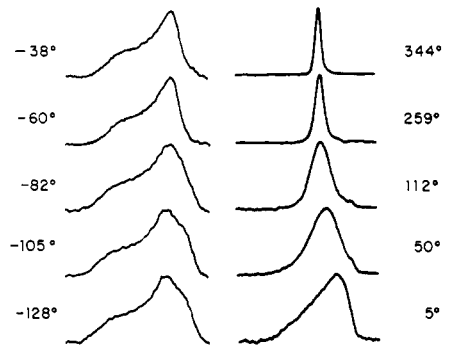

Figure 10. ^{19}F REV-8 chemical shift line shapes of the amorphous fraction of melt-recrystallized PTFE at various temperatures.

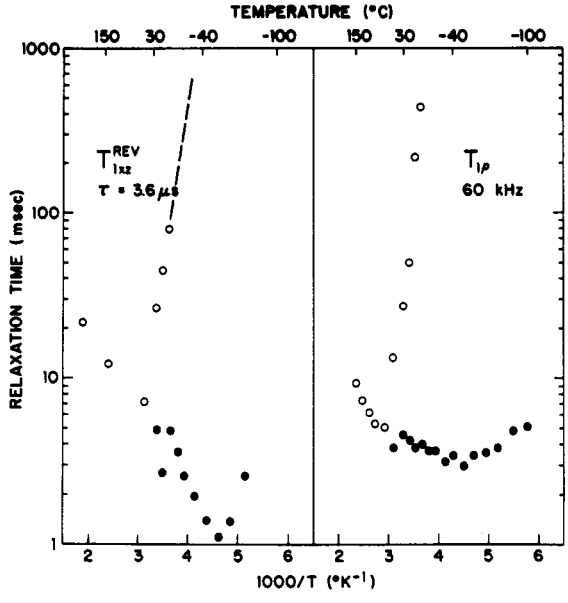

Figure 11. Temperature dependence of the $T_{1\rho}$ and T_{1xz}^{REV} relaxation times of a 68% crystalline melt-recrystallized PTFE sample. Solid circles denote the short relaxation time component in a double-exponential decay. T_{1xz}^{REV} times longer than 100 ms and $T_{1\rho}$ times longer than 1 s are not shown since their experimental values could not be determined accurately. The expected T_{1xz}^{REV} temperature dependence below 15 °C is indicated by the broken line.

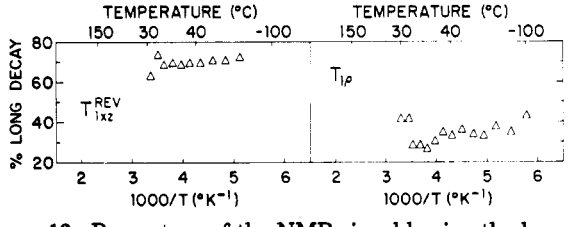

Figure 12. Percentage of the NMR signal having the long relaxation time in a double-exponential T_{1xz}^{REV} or $T_{1\rho}$ decay (see Figure 11) for a 68% crystalline melt-recrystallized PTFE sample.

data show two components in the relaxation data below 30 °C. These are represented by the filled and unfilled circles in the figure. Above 30 °C the relaxation decays are singly exponential. The relative contributions of the long component in the decays are plotted in Figure 12. (These numbers as well as the values for the relaxation times were obtained by a computer fit of the experimental data.) Clearly, the fractions with the long and short relaxation times represent the crystalline and amorphous phases, respectively. Figure 12 illustrates that the relative amounts of the decays in the T_{1xz}^{REV} measurements are more representative of the two phases than are the $T_{1\rho}$

measurements. The components of the T_{1xz}^{REV} decay are more representative of a single phase than the $T_{1\rho}$ measurements because the multiple-pulse measurement suppresses spin diffusion which severely complicates the interpretation of $T_{1\rho}$ measurements.[20] Similar measurements of melt-recrystallized PTFE samples of different crystallinity gave essentially the same results for the relaxation times.

The amorphous T_{1xz}^{REV} and $T_{1\rho}$ minima occur at approximately the same temperature where the amorphous line shape narrows into an axially symmetric pattern, indicating that these phenomena are related to the same macromolecular process. The crystalline T_{1xz}^{REV} and $T_{1\rho}$ relaxation times approach a minimum at 30 °C, which is clearly related to the line-shape changes shown in Figure 8. As is shown in Appendix C, we expect a T_{1xz}^{REV} minimum when the torsional diffusion rate is 18 kHz. Indeed, the diffusion rates determined from the crystalline line shapes (Figure 9) extrapolate to a rate of 18 kHZ at ~35 °C. This agreement quantitatively establishes that the same macromolecular process is responsible for both the crystalline chemical shift line-shape changes near 20 °C and the T_{1xz}^{REV} minimum near 30 °C.

The single-exponential T_{1xz}^{REV} and $T_{1\rho}$ decays above the first-order phase transition at 30 °C are not accompanied by related chemical shift line-shape changes: the crystalline line shape does not change and, as we will explain shortly, the narrowing of the amorphous line shape at high temperature cannot be directly related to the observed relaxation times. Most peculiar is the fact that, although the crystalline and amorphous line shapes are significantly different at higher temperatures, the relaxation times in the radio-frequency interaction frame are identical in the two phases. This probably indicates that the same dynamical process dominates the relaxation rate in both phases.

The line shape of the amorphous fraction (shown in Figure 10) is seen to be changing from that of a chemical shift tensor of axial symmetry at −38 °C to one with spherical symmetry near the melting point. Hence, the anisotropic reorientation at low temperatures gradually changes into an essentially isotropic reorientation at high temperatures. As is often the case with magnetic resonance line-shape phenomena of this kind, one might suppose that this isotropic motion already exists at a slow rate at the lowest temperatures and that the increase of the rate with increasing temperature is reflected by the variations in the line shape. In the case of the amorphous PTFE line shapes, this would imply that above 50 °C the line shapes were Lorentzian and *homogeneously* broadened (fast-motion limit). However, this would also imply that the relaxation time T_{1xz}^{REV} be equal to the inverse half-width of the Lorentzian line. (This has recently been shown theoretically and experimentally for a chemical-exchange case.[21]) Since in our case T_{1xz}^{REV} is 2 orders of magnitude longer than the inverse line width, we must conclude that the line shapes are *inhomogeneously* broadened. Further evidence that this broadening is due to chemical shift inhomogeneity was obtained by recording the spectra further off resonance, which led to narrowing of the spectra. This narrowing quantitatively agreed with the experimentally observed nonlinearity of the scaled offset frequency which is characterized by smaller chemical shift scaling factors for larger offsets. If the broadening were the result of spurious dipolar interactions, we would have observed wider lines further off resonance. The correct description of the amorphous line shapes is that reorientational motion takes place at a rate fast compared to the chemical shift range in question (10 kHz) and that the angular *amplitude* rather than the *rate* of this motion grows with increasing temperature until essentially isotropic motion is achieved at the melting point. In the Discussion section of this paper we will present a statistical model for this dynamic behavior.

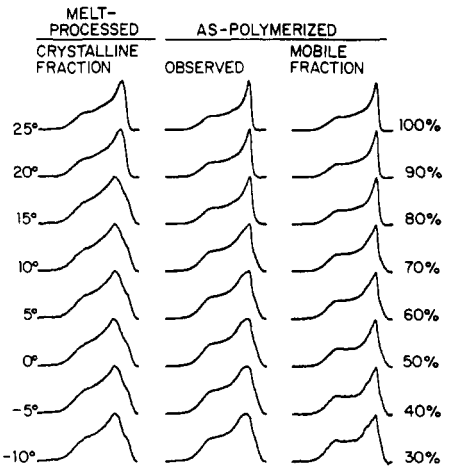

Figure 13. ^{19}F REV-8 chemical shift line shapes of as-polymerized PTFE (center) and the crystalline fraction of melt-recrystallized PTFE (left). The as-polymerized spectra can be considered as linear combinations of the spectra in the left and right columns, where the percentages indicate the relative contributions of the latter.

Additionally, we have attempted to determine if any molecular weight dependence can be observed. Samples of melt-recrystallized PTFE of low (MW $\simeq 0.5 \times 10^6$), medium (MW $\simeq 5 \times 10^6$), and high (MW $\simeq 200 \times 10^6$) molecular weight were used to obtain chemical shift spectra and T_1 and $T_{1\rho}$ relaxation times, and no differences could be detected.

Virgin and Annealed Virgin PTFE. As-polymerized PTFE and PTFE heat treated below the melting point do not exhibit the same general NMR behavior found for the melt-recrystallized samples. Particularly, the REV-8 line shapes of virgin PTFE below 30 °C deviate substantially from the decomposed crystalline spectra obtained from melt-recrystallized samples (see Figure 13), although virgin PTFE is 99.7% crystalline, as determined from REV-8 spectra above 30 °C. Moreover, the $T_{1\rho}$ and T_{1xz}^{REV} decays of a 97% crystalline, annealed virgin sample are nonexponential. The results of a two-component analysis of these decays are shown in Figures 14 and 15. The large scatter in the short T_{1xz}^{REV} values is probably a result of the small amount of short decay in the signal. Highly significant, however, is that the percentage of the signal relaxing with a short T_{1xz}^{REV} sharply increases from less than 20% at −30 °C to almost 70% at 20 °C (Figure 15). Since the sample is almost 100% crystalline, this indicates that the polymer below 30 °C consists of more than one crystalline-like phase, where the fraction with higher molecular mobility appears to grow as the temperature increases. The REV-8 virgin-polymer line shapes are composed of two components, one being identical with the crystalline line shape of melt-recrystallized PTFE and the other corresponding to PTFE molecules which undergo torsional motion at lower temperatures. The results of a line-shape decomposition are also shown in Figure 13. The percentages chosen for the relative contributions of the two observed fractions are highly subjective and have an inaccuracy of about ±20%. From the line shapes of the more mobile portion we estimate (in a way similar to the line-shape analysis in Figure 8) a torsional diffusion rate of at least 1 kHz at −10 °C.

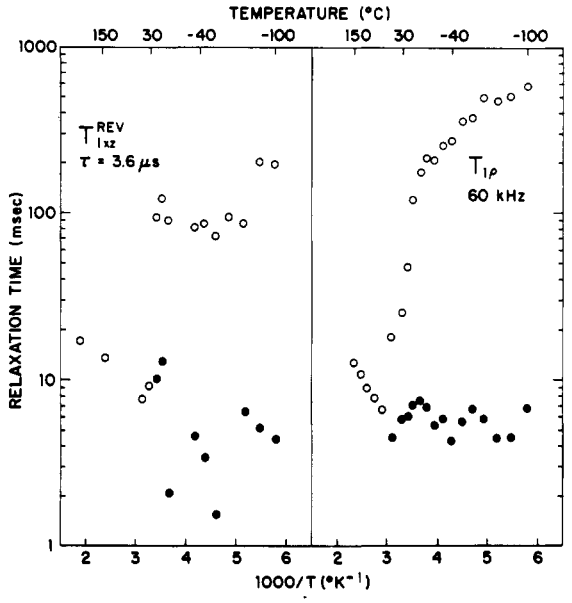

Figure 14. Same as Figure 11, for a 95% annealed virgin PTFE sample.

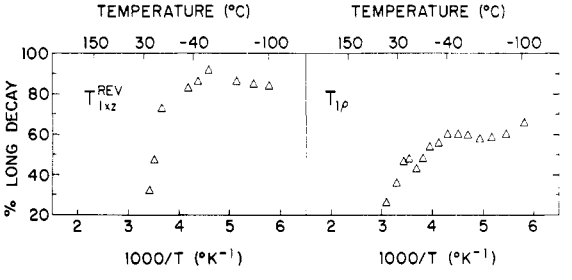

Figure 15. Same as Figure 12, for a 95% annealed virgin PTFE sample.

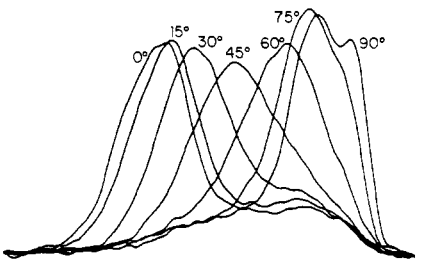

Figure 16. ^{19}F REV-8 spectra of oriented PTFE fibers at −108 °C for various angles between the fiber direction and the magnetic field.

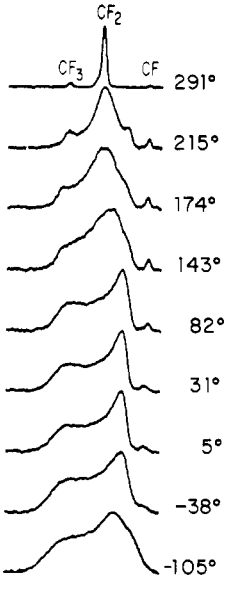

Figure 17. ^{19}F REV-8 spectra of a copolymer of TFE and HFP at various temperatures.

PTFE Fibers. The use of chemical shift spectra for the study of randomly oriented solid samples has the advantage that the line shapes are inhomogeneously broadened in such a way that different portions of the spectrum correspond to distinctly oriented molecular species. This allows us to obtain detailed orientational information concerning molecular structure and dynamics. However, we would expect to obtain the same information more directly from chemical shift spectra of samples in which the molecules are aligned. For that reason we obtained REV-8 spectra of a PTFE fiber sample at various temperatures and orientations. Figure 16 shows a superposition of some of these spectra taken at −108 °C, with different orientations. The spectra consist of a narrow component whose position is dependent upon orientation (aligned molecules) and a broad, orientation-independent component (randomly oriented molecules). The randomly oriented material constitutes 25% of the spectra and could be corrected for by numerically subtracting the line shape of unoriented PTFE at the same temperature. The high-temperature line shape of a randomly oriented sample of chopped fiber showed an amorphous content of 32%. The difference between this percentage and the 25% of unoriented material at −108 °C is well beyond experimental uncertainty and suggests that part of the amorphous polymer is aligned at low temperatures.

A least-squares analysis of the line shapes of the oriented fiber material shows that the alignment of the macromolecular axis is not complete but has an angular distribution with a standard deviation of about 11° (provided the distribution is Gaussian). Furthermore, partial information concerning the angular positioning of the ^{19}F chemical shift tensor with respect to the molecular geometry is obtained (see Appendix B).

The qualitative behavior of the fiber line shapes as a function of temperature is consistent with the model of torsional reorientation about the molecular chain axis, particularly in the 0–30 °C temperature range. Unfortunately, a quantitative analysis of the motional process is fruitless, since the details of the line shape depend strongly on the exact angular distribution profile of the molecular chain axes (unknown). Thus the advantages of having an oriented sample are to a large extent outweighed by the disadvantage of the inherent uncertainty in the degree of alignment.

TFE/HFP Copolymers. We have also obtained chemical shift spectra of a copolymer of tetrafluoroethylene and hexafluoropropylene (TFE/HFP; 8.5 mol % HFP).[14] Figure 17 shows representative chemical shift spectra as a function of temperature. These spectra illustrate that the observed line shapes are qualitatively similar to those obtained for PTFE in that CF_2 groups in crystalline and amorphous regions are observed and in addition CF_3 and CF line shapes are observed. It is apparent from Figure 17 that the motion of the CF groups appears to be fast by ~100 °C while the CF_3 groups do not indicate the presence of isotropic motion below 200 °C. This indicates that backbone reorientation is rapid (≳10 kHz) by ~100 °C but CF_3 group internal rotation is not rapid below 200 °C.

The part of the TFE/HFP copolymer line shape corresponding to CF_2 groups can be analyzed above 50 °C by subtracting the PTFE crystalline line shape from these spectra until a visual inspection indicates that the proper amount has been subtracted. The resulting line shape

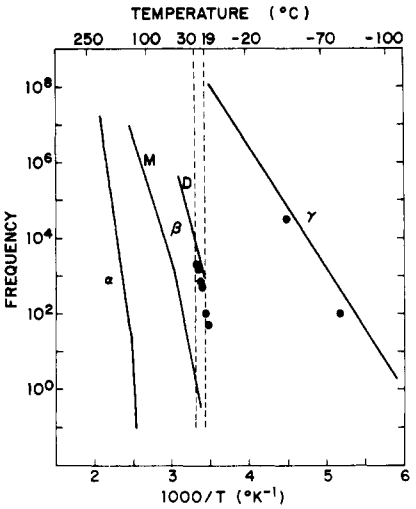

Figure 18. Relaxation map of PTFE. The full lines indicate the approximate temperature dependence of the α, β, and γ relaxation frequencies determined by dynamic mechanical and dielectric measurements.[4,21] Two branches have been observed in the β relaxations: M (dynamic mechanical and dielectric data) and D (dielectric data only). The vertical broken lines represent the crystalline-phase transitions. The solid circles are the results of this work: The points near 19 °C represent the rotational diffusion rate of the molecules in the crystalline regions (Figure 9). The points at -50 and -80 °C are based on the T_{1xz}^{REV} and $T_{1\rho}$ minima and the amorphous chemical shift line shapes, respectively (see text).

contains CF_3 and CF line shapes plus the CF_2 amorphous line shape. This procedure is subject to larger errors than the analysis used for the PTFE line shapes but does indicate that one-third of the CF_2 groups are in a crystalline environment.

The amorphous CF_2 line shapes obtained by this procedure can be analyzed in the same fashion as the PTFE amorphous line shapes to give insight into the type of macromolecular motion present (see Discussion).

Discussion

PTFE is known to undergo two crystalline first-order transitions at 19 and 30 °C and three viscoelastic relaxations have been observed. The temperature dependence of the relaxations (α, β, γ), as determined by dielectric and anelastic measurements, is shown in the relaxation map of Figure 18 along with the temperatures of the crystalline-phase transitions (vertical dotted lines).[22-24] Also indicated in Figure 18 are the results of rotational diffusion rates obtained in this study. The γ relaxation is thought to occur in the amorphous regions and has an activation energy E_a = 18 kcal/mol.[17] The β relaxation occurs in the crystalline regions and is related to reorientation about the chain axis and has E_a = 34 kcal/mol.[17] The α relaxation has an E_a = 88 kcal/mol[17] and may involve the crystalline and/or amorphous regions. The crystalline transition at 19 °C corresponds to uncoiling the helical structure from a repeat distance (180° twist) of 13 carbon atoms to a repeat distance of 15 carbon atoms.[22-24] The crystalline transition at 30 °C is attributed to further uncoiling of the helical chain. The onset of translational displacement along the chain axis begins above 30 °C and complete translational disorder is observed by 160 °C.[22-24]

The chemical shift line-shape changes observed for the crystalline fraction of melt-recrystallized PTFE are due to reorientation about an axis essentially parallel to σ_{zz} (which is tilted ~12° from the molecular chain axis). This process has an activation energy of 48 ± 11 kcal/mol (Figure 9). In addition, the $T_{1\rho}$ and T_{1xz}^{REV} relaxation data (Figure 11) show minima near 30 °C, where the rotational diffusion rate from Figure 9 is approximately equal to the effective spin-locking field (see Appendix C). These three facts indicate that the process responsible for the line-shape changes in crystalline regions is a relaxation process that can be described as a reorientation about the chain axis that increases in rate with increasing temperature. This process is clearly the β relaxation. The relaxation rates determined by NMR are in good agreement with some of the previous dielectric results (Figure 18). The activation energy found from these NMR results is also in good agreement with some of the dielectric results but disagrees with the often-quoted value of 34 kcal/mol. Translational displacements along the chain axis in well-ordered crystalline regions (which have been previously observed[22-24]) would not give rise to any observable change in the chemical shift spectra.

The β relaxation process that we observe overlaps the crystalline-phase transition at 19 °C. This suggests that the 19 and 30 °C phase transitions are intimately connected with the β relaxation. In other words, the uncoiling of the chain axis that occurs during these phase transitions and the reorientation (torsional motion) about the chain axis (β relaxation) occur simultaneously and are probably interdependent.

The line-shape changes observed for the amorphous fraction of the polymer between -128 and -60 °C indicate some type of relaxation whose origin is similar to that just described. It appears that this process involves reorientation about the local chain axis and the rate of this process is ~0.1 kHz at ~-80 °C (from a comparison of the -82 °C amorphous spectrum in Figure 7 to the 0.1-kHz calculated spectrum in Figure 8). The relaxation data indicate that the rate of this motion is ~30 kHz at -50 °C (see Appendix C). However, this process is coupled with a higher temperature process (see below) and does not give definitive line shapes which are amenable to line-shape analysis. We can estimate that this relaxation has an activation energy of 16 ± 5 kcal/mol. Therefore, we conclude that the process responsible for these results is the γ relaxation.

The relaxation times shown in Figure 11 indicate that from -128 to 300 °C only two minima are observed. These two minima are associated with the γ and β relaxations previously observed in anelastic and dielectric measurements. We see no evidence of any other relaxations on the time scale of $T_{1\rho}$ and T_{1xz}^{REV} (10–100 kHz). Therefore, these NMR experiments as well as earlier NMR experiments[4] do not detect the α relaxation. Furthermore, the reorientational motion of the amorphous chain direction (see below) cannot be identified with the α relaxation since this motion involves rates faster than 100 MHz below room temperature while the α relaxation is slower than 1 Hz below 100 °C.

The rate of the molecular motion responsible for the observed amorphous line-shape changes above -40 °C must be much less than or much greater than 1–10 kHz (T_{1xz}^{REV}) and much less or much greater than 100 MHz (T_1) from -40 to 260 °C[25] since no minimum was observed in the relaxation data. In addition, the rate must be ≳1–10 kHz to cause the observed line-shape changes. Therefore, the rate must be greater than 100 MHz. Also, the chemical shift spectrum is not homogeneously broadened below 260 °C as would be required of an isotropic exchange process to cause the observed line-shape changes. These two considerations lead us to conclude that the process responsible for the observed line-shape changes may be idealized as one in which *the rate of the motion is fast*

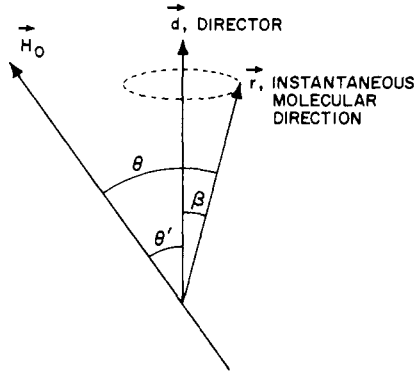

Figure 19. Definition of angles describing the relative orientations of the magnetic field ($\vec{H}_0$), the instantaneous molecular direction ($\vec{r}$), and the average molecular direction ($\vec{d}$) in a dynamically disoriented system. In amorphous PTFE $\vec{r}$ represents the instantaneous chain direction and $\vec{d}$ the local director.

(≳100 MHz) at all temperatures (-40 to 260 °C) and the amplitude of the motion grows as a function of temperature. Since the chemical shift line shape is nearly axially symmetric at ~-68 °C, we can describe this motion whose amplitude grows with temperature as reorientation of the local chain axis.

The reorientation of the local chain axis gives rise to the partial narrowing of the amorphous REV-8 spectra and is of a random nature. In a short period of time, a particular segment of the macromolecular chain assumes a distribution of directions which deviate from its orientation at rest. In analogy to the description of molecular ordering in liquid crystals,[26] we use the concept of a local-order parameter for the quantitative characterization of the extent of these fluctuations.

In liquid crystals, the order parameter, S_β, is a well-defined parameter for the characterization of NMR spectra where very fast reorientational motion of the molecules gives rise to a uniform scaling (with a factor S_β) of spectral quantities such as nuclear dipolar splittings.[26-28,39] This uniform scaling is obtained in liquid crystals because the following three conditions are satisfied: (i) The term in the nuclear spin Hamiltonian being averaged by the fast motion is proportional to $(3\cos^2\theta - 1)$, where θ is the angle between the magnetic field $\vec{H}_0$ and an instantaneous molecular vector $\vec{r}$ (see Figure 19). (ii) The distribution of the orientations sampled by the vector $\vec{r}$ during the motion is axially symmetric with respect to a local director $\vec{d}$. (iii) All the molecules in the sample reorient identically; i.e., the distribution $P(\beta)$ of the angles β between the instantaneous molecular vectors $\vec{r}$ and their local average direction $\vec{d}$ is the same for all molecules. Since the motion is very fast, an NMR spectrum is observed which is proportional to the average value $\langle 3\cos^2\theta - 1\rangle$, and if the above conditions are fulfilled, we have the relationship

$$\langle 3\cos^2\theta - 1\rangle = S_\beta(3\cos^2\theta' - 1) \tag{1}$$

where

$$S_\beta = \tfrac{1}{2}\langle 3\cos^2\beta - 1\rangle = \frac{\int \tfrac{1}{2}(3\cos^2\beta - 1)P(\beta)\sin\beta\,d\beta}{\int P(\beta)\sin\beta\,d\beta} \tag{2}$$

θ' being the angle between the director $\vec{d}$ and the magnetic field $\vec{H}_0$.

In the amorphous regions of PTFE we identify $\vec{d}$ with the time average of the local chain direction and $\vec{r}$ with its instantaneous direction. Since the torsional motion about the chain axis above -68 °C is such that we retain effective axial symmetry of the chemical shift with respect to the molecular chain axis, we do have the angular dependence required by condition i

$$\sigma = \sigma_{iso} + \tfrac{1}{3}\Delta\sigma(3\cos^2\theta - 1) \tag{3}$$

where

$$\sigma_{iso} = \tfrac{1}{3}(\sigma_\parallel + 2\sigma_\perp) \tag{4}$$

$$\Delta\sigma = \sigma_\parallel - \sigma_\perp \tag{5}$$

If conditions ii and iii were also satisfied, we would have observed a line shape corresponding to an axially symmetric chemical shift tensor to near the melting point and we would have calculated an unambiguous value for the order parameter from

$$S_\beta(T) = \Delta\sigma(T)/\Delta\sigma(T_0) \tag{6}$$

where $\Delta\sigma(T)$ is the line width at temperature T and T_0 is the temperature at which the amplitude of the motion is effectively zero. However, as can be seen in Figure 10, the line shape is essentially symmetric above 50 °C. This is most likely due to the facts that the chain-bending motion is not really symmetrically distributed about the director and that molecules in different sites of the polymer have different amplitudes of motion, giving rise to a distribution of order parameters. Nevertheless, we feel that the observed width of the narrowed line is very closely related to an order parameter which corresponds to some kind of average value for $S_\beta = \tfrac{1}{2}\langle 3\cos^2\beta - 1\rangle$. Experimental values for $\Delta\sigma$ were obtained by least-squares curve fitting of the amorphous line shapes at temperatures above -40 °C to an axially symmetric chemical shift tensor. From these values S_β was calculated with eq 6, where $\Delta\sigma(T_0)$ was taken as the $\Delta\sigma$ of the crystalline spectra above room temperature. Figure 20 gives the temperature dependence of the local-order parameter obtained in this fashion for the amorphous regions in PTFE and in the TFE/HFP copolymer.

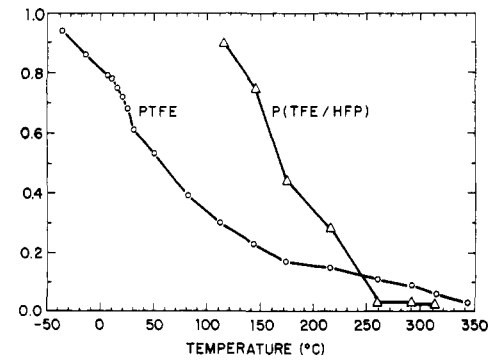

Figure 20. Temperature dependence of the local-order parameter, S_β, of the fluctuating chain directions in the amorphous regions of PTFE and a TFE/HFP copolymer.

We can now *speculate* as to the molecular nature of this reorientational motion of the PTFE backbone in the amorphous state. We assume that our experimentally determined order parameters closely represent the average value of $\tfrac{1}{2}\langle 3\cos^2\beta - 1\rangle$ of all the molecular chains in the amorphous regions.

Two models for the dynamic distribution of angular displacements β are considered. The first is a Gaussian distribution, $P(\beta) \propto \exp(-\beta^2/2\beta_0^2)$, which is characterized by a root-mean-square angle or standard deviation β_0. Substitution of this expression for $P(\beta)$ in eq 2 provides the dependence of S_β as a function of β_0 and thus allows

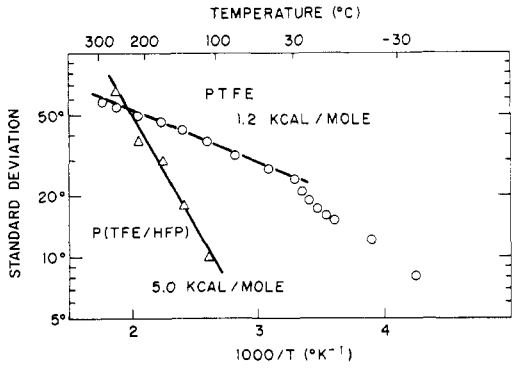

Figure 21. Temperature dependence of the root-mean-square value of a Gaussian distribution of the amplitude of chain-axis fluctuations in the amorphous regions of PTFE and a TFE/HFP copolymer.

the determination of the temperature dependence of β_0.[27] These results are shown in Figure 21. It is seen that the magnitude of the angular disorder in the amorphous regions at the crystalline melting point is of the order of 60°.

The temperature dependence of the standard deviation of the fluctuations can be related to the potential energy required to introduce disorder into the polymer chain. Figure 21 shows a linear dependence of log β_0 on $1/T$ over a fairly large temperature range. This suggests that higher energy chain conformations are populated according to a Boltzmann distribution. From the slope of the line in Figure 21 we deduce a potential energy difference ΔE = 1.2 kcal/mol for the creation of local disorder in the backbone of amorphous PTFE. A comparison of this ΔE to values predicted by the four-state rotational model of Bates and Stockmayer[29] (where $t^{\pm}t^{\pm}$ is the ground state) shows reasonable agreement with their values for $t^{\pm}g^{\pm}$ defects (ΔE = 1.4 ± 0.4 kcal/mol) or $t^{\pm\mp}$ defects (ΔE = 1.1 ± 0.7 kcal/mol). In addition, this value for the potential energy difference is essentially identical with that found from infrared studies of PTFE, which postulated the existence of helix reversals ($t^{\pm}t^{\mp}$).[30-32] However, since helix reversals are unlikely to be responsible for large reorientations of the chain axis, the motion that we observe is more likely due to $t^{\pm}g^{\mp}$ defects. On the other hand, our model of a continuous Gaussian distribution is obviously not compatible with discrete conformational changes in the backbone. Instead, it may possibly be related to large amplitude anharmonic vibrations. Indeed, we have established that the macromolecular motion is of a high frequency (≳100 MHz). This vibration could be a perturbed longitudinal acoustic mode and may be detectable with Raman spectroscopy at low temperatures, where the concentration of defects may be small enough so as to not cause the Raman band to be so broad as to be unobservable.[33,34]

A second model to explain the growing dynamic disorder with increasing temperature is directly related to the creation of gauche conformations in the predominantly trans configuration PTFE chain. In this model, the angle β can have essentially one of two distinct values: $\beta_0 = 0$ in the case of an undeformed chain, and $\beta = \beta_k$ in parts of the chain that are bent away from their original direction due to the creation of a kink. An analysis of the PTFE molecular geometry shows that $\beta_k = 56 \pm 4°$ for a trans–gauche conformational change.[7,24] If the number of CF_2 groups in kinks is p times the number of CF_2 groups in undeformed parts of the chain, then

$$S_\beta = [\tfrac{1}{2}(3\cos^2\beta_0 - 1) + \tfrac{1}{2}p(3\cos^2\beta_k - 1)]/(1 + p)$$
$$\simeq 1/(1 + p)$$

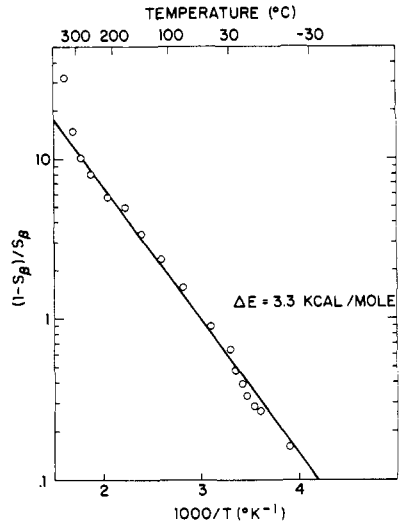

Figure 22. Temperature dependence of $p = (1 - S_\beta)/S_\beta$, S_β being the local-order parameter in the amorphous regions of PTFE. This quantity is related to the population of kinks (see text).

If the ratio p follows a Boltzmann temperature dependence then

$$(1 - S_\beta)/S_\beta \simeq p \sim \exp(-\Delta E/kT)$$

Figure 22 shows a surprisingly good agreement with this model. The corresponding potential energy for the creation of chain kinks is ΔE = 3.3 kcal/mol. This is more than twice the value of 1.4 kcal/mol predicted by Bates and Stockmayer[29] for the introduction of a gauche conformation and may be due to the fact that a kink requires at least two gauche conformations in order to maintain the overall chain position in the polymer matrix. The preexponential factor corresponds to the statistical weight of deformed chain segments relative to undeformed segments. From the data plotted in Figure 22 we find $p_0 \sim 300$. This value seems somewhat high but is perhaps not too surprising if we realize how many chain segments in a random coil are not parallel to a certain fixed orientation.

Additionally, a Reneker-type[35] defect is suggested by the potential energy difference found for this second model since the calculated energy required for the formation of this type of defect in amorphous polyethylene is ≃4 kcal/mol[35] (poly(tetrafluoroethylene) should be similar). This defect model is also attractive in that it provides a mechanism for establishing a correspondence between the chain-axis translation observed in crystalline PTFE by X-ray[36] (which is consistent with our results) and a translation (longitudinal motion) of the local chain axis in the amorphous regions ("reptation").[37] Since the chain axis is "straight" in the crystalline regions but not in the amorphous regions, segmental reorientation occurs only in the latter and is reflected in our results. We find this an attractive possibility because it explains why we observe the same $T_{1\rho}$ and T_{1xz}^{REV} relaxation times for the amorphous and the crystalline signals above 30 °C. It also agrees with the diminished sharp features of the crystalline line-shape component of highly amorphous PTFE (see the high-temperature spectra in Figures 2, 7, and A-1). This could be explained as a chemical-exchange effect of reptating chains into and out of the relatively small crystallites.

We certainly do not pretend that any of the motional models mentioned in this discussion of the amorphous local chain axis fluctuations are exact. However, it is clear that an increase of the amplitude of dynamic chain disorder is present in amorphous PTFE. In general, large-amplitude

high-frequency macromolecular motions may be the origin of the problem found in correlating the results of broad-line NMR studies and NMR relaxation measurements. Both measurements may be dominated by a growth in the amplitude of the motion (the amount of the second moment which is modulated by the motion) rather than an increase in the rate of the motion. We have observed this to be the case in poly(ethylene terephthalate) and we will report these results in the near future. A similar behavior has recently been reported for the deuterium NMR of polyethylene,[38] where the temperature dependence of the width of the amorphous line very closely resembles our chemical shift spectra of PTFE.

Virgin and annealed virgin PTFE have nonamorphous NMR line shapes above 25 °C identical with those found for the crystalline fraction of melt-recrystallized samples. Below 25 °C, these results show that virgin PTFE is composed of at least two types of crystalline polymer with different rates of motion. The two forms become indistinguishable when they are rapidly reorienting about their chain axes. Additional evidence for the presence of more than one type of crystalline phase has been given by Eby,[17] where the temperature dependence of the temperature derivative of the modulus ($\partial M/\partial T$) was found to be much more diffuse for virgin polymer than melt-recrystallized polymer. This observation as well as our observations could be related to a larger distribution of segment lengths in virgin than in melt-recrystallized polymer.[17]

The chemical shift line shapes obtained for the TFE-HFP copolymer illustrate the same types of motion as observed in PTFE. The CF_2 groups in the crystalline fraction of the polymer are rapidly reorienting about their chain axes by −40 °C and the CF_2 groups in the amorphous fraction of the polymer show reorientation of the local chain axis at temperatures ≤100 °C. These amorphous line shapes can be analyzed in terms of an order parameter (Figure 20) and the amplitude of the chain-axis fluctuations to yield a potential energy difference (first model) for introducing local backbone disorder of 5.0 kcal/mol (Figure 21). This potential energy difference is much larger than that found for PTFE (1.2 kcal/mol) and indicates that the presence of sterically larger CF_3 groups in the copolymer hinder chain-axis reorientation. In addition, we note that the CF groups show evidence of motion above 100 °C due to backbone reorientation; however, rapid internal rotation of the CF_3 group is not observed until ~250 °C. Previous conventional NMR results[39] have shown the absence of CF_3 rotation up to 200 °C.

Summary

Chemical shift NMR spectra have been used to obtain information about specific macromolecular motions in randomly oriented PTFE and poly(TFE/HFP). The β relaxation is confirmed to involve reorientation of CF_2 groups about the chain axis in crystalline PTFE. The activation energy is in reasonable agreement with previous anelastic and dielectric relaxation measurements[22] and the relaxation mechanism agrees with that found by X-ray[24] and NMR[3,39] methods using oriented specimens. The α relaxation is not observed in these or conventional NMR experiments.[4] The γ relaxation is confirmed to take place in the amorphous regions and the activation energy is in reasonable agreement with previous anelastic and dielectric relaxation results.[22] Rapid chain-axis reorientation in the amorphous regions of PTFE is characterized by an increasing amplitude of motion with increasing temperature; the most attractive model is a Reneker-type defect. Insertion of CF_3 groups into the backbone has three discernible effects: rapid reorientation about the chain axis in crystalline regions occurs at lower temperatures, the CF_3 groups inhibit chain-axis reorientation in the amorphous regions, and the CF_3 groups do not internally rotate until ~250 °C. Virgin PTFE is 99.7% crystalline and the crystalline fraction is composed of two different types of crystalline polymer that are distinguished by their relative mobility. There is no discernible effect of molecular weight upon any of these results.

Acknowledgment. We are much indebted to the late Professor R. W. Vaughan for valuable advice and his constant enthusiasm. We gratefully achnowledge discussions with Dr. C. A. Sperati and Dr. H. W. Starkweather and the skilled technical assistance of R. O. Balback.

Appendix A. Numerical Decomposition of Line Shapes into Crystalline and Amorphous Fractions

The decomposition of the REV-8 line shapes of PTFE into crystalline and amorphous constituents is based on the assumption that the line shapes are linear combinations of not more than two components. Another assumption made in the numerical analysis of the line shapes is that the crystalline and amorphous line shapes are identical for samples with different crystallinities. To verify these assumptions we chose the most crystalline (c) and most amorphous (a) spectra as reference line shapes and determined for any other sample (x) the coefficients χ' and α' which gave a least-squares computer fit to the equation

$$x(\omega) = \chi' c(\omega) + \alpha' a(\omega)$$

Invariably, we found that the sum of the parameters χ' and α' was equal to 1.00 ± 0.01 at temperatures above 30 °C, where the line shapes are significantly different. The results of this line-fitting procedure demonstrate that our two-component model has a high degree of physical reality (see Figure A-1). The only significant deviation from this model is observed in the most amorphous samples above 250 °C, where the line shapes are slighlty distorted, possibly because of chemical exchange between the amorphous and crystalline regions. Although the multiple-pulse experiment introduces a line broadening which varies as a function of offset frequency and dipolar interaction,[12,16] we have experimentally established that the integrated intensity is independent of these parameters. Hence, the coefficients χ' provide a quantitative measure of the degree of crystallinity. On an arbitrary scale where sample a is 0% and c is 100%, we define χ' as the *relative crystallinity* of sample x. If χ_c, χ_a, and χ are the *absolute crystallinities* of the respective samples, then $\chi = \chi'\chi_c + \alpha'\chi_a$.

There is no numerical method which independently determines χ_c and χ_a. However, by visual examination of linear combinations of spectra a and c we determined the absolute crystallinities to be $\chi_c = 97 \pm 1\%$ and $\chi_a = 40 \pm 5\%$. The crystallinities plotted in Figures 4 and 5 are calculated from these values for χ_c and χ_a and the computer-fitted relative crystallinities χ' (2% uncertainty). Thus, the plot of the percent crystallinity vs. the temperature in Figure 5 actually represents the temperature independence of the more accurately determined relative crystallinity.

The pure amorphous (A) and crystalline (C) line shapes used for subsequent motional analysis are calculated by numerical solution of the equations

$$c(\omega) = \chi_c C(\omega) + (1 - \chi_c)A(\omega)$$

$$a(\omega) = \chi_a C(\omega) + (1 - \chi_a)A(\omega)$$

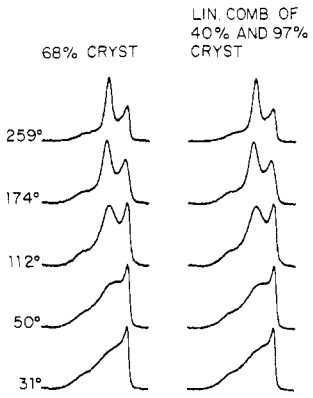

Figure A-1. ^{19}F REV-8 chemical shift spectra of 68% crystalline PTFE and linear combinations of line shapes of 40% and 97% crystalline PTFE.

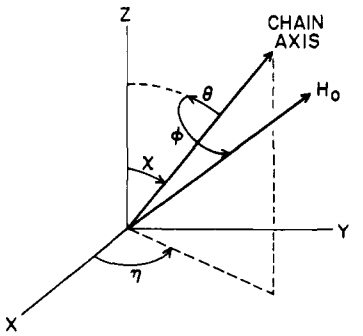

Figure B-1. Definition of the angles describing the relative orientations of the polymer chain axis, the magnetic field (H_0), and the principal ^{19}F chemical shift tensor axes (x = 178, y = 141, z = 41 ppm). The H_0 direction is characterized with respect to the polymer chain axis by a polar-angle rotation θ toward z followed by an azimuthal rotation ϕ.

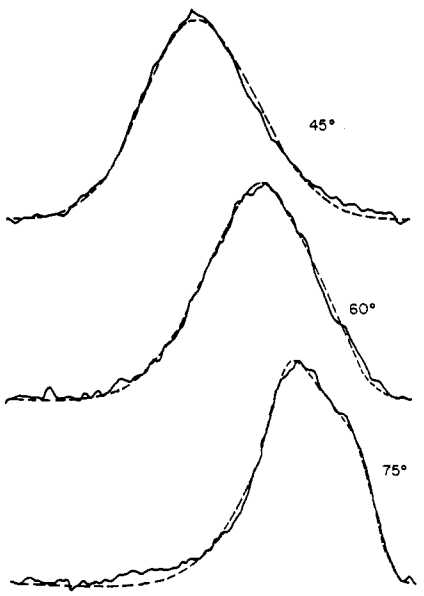

Figure B-2. Experimental (full line) and calculated (broken line) ^{19}F REV-8 chemical shift spectra of PTFE fibers at −108 °C for various orientations with respect to the magnetic field. The experimental line shapes are corrected for 25% unoriented material.

When applied to the melt-recrystallized PTFE samples at temperatures below 30 °C, the method of linear combination yields essentially the same crystallinity as at higher temperatures, although with larger uncertainties.

Appendix B. Chemical Shift Tensor Components Determined from Powder and Oriented Fiber Samples

Chemical shift powder patterns measured by multiple-pulse techniques are complicated by such effects as nonlinear scaling factors and nonuniform line broadenings. The scaling factors were experimentally determined (see Experimental Section) while the line broadening (w) was assumed to be Lorentzian with a quadratic dependence on the offset frequency (f_{os})

$$w = w_0 + w_1 f_{os} + w_2 f_{os}^2 \quad \text{(B-1)}$$

This quadratic behavior is in agreement with predicted dipolar-offset cross terms in the average Hamiltonian[16] and was also observed in CaF_2 (100) REV-8 spectra taken under the same conditions. The principal values of the chemical shift tensor and the line-broadening coefficients were determined by a least-squares fit of the observed line shape to a calculated powder pattern, while taking the nonlinear scaling factor into account. The results for the principal values of the chemical shift tensor of the spectrum taken at −128 °C are 178, 141, and 41 ppm with respect to liquid $CFCl_3$. The axially symmetric crystalline line shapes at high temperatures gave 156, 156, and 49 ppm. These values agree with previous results.[6-8]

Since the transition from the low-temperature tensor to the high-temperature crystalline tensor undoubtedly results from reorientation about the molecular chain axis, we can use these chemical shift results to obtain partial information about the alignment of the ^{19}F shift tensor with respect to the molecular frame; i.e., we can estimate the polar angles, χ and η, of the chain-axis direction in the principal axis system of the shift tensor (see Figure B-1). If the principal shift components of the rigid tensor are σ_{xx}, σ_{yy}, and σ_{zz}, and those of the averaged tensor are $\sigma_{\parallel}$, and $\sigma_{\perp}$, then

$$\sigma_{\parallel} - \sigma_{\perp} = \tfrac{1}{2}\Delta\sigma(3\cos^2\chi - 1) + \tfrac{3}{4}\delta\sigma\sin^2\chi\cos^2\eta \quad \text{(B-2)}$$

where

$$\Delta\sigma = \sigma_{zz} - \tfrac{1}{2}(\sigma_{xx} + \sigma_{yy}) \quad \text{(B-3)}$$

$$\delta\sigma = \sigma_{xx} - \sigma_{yy} \quad \text{(B-4)}$$

From the experimental shift components we then derive that the angle between the σ_{zz} axis and the polymer chain direction lies between $\chi = 14 \pm 4°$ (if $\eta = 0°$) and $\chi = 16 \pm 4°$ (if $\eta = 90°$).

For the case of a completely aligned fiber sample we have a single experimentally determined value for the angle θ between the field H_0 and the polymer chain direction, while the azimuthal angle ϕ takes random values between 0 and 360° (see Figure B-1). In order to calculate chemical shift line shapes for this situation we need to express the shift as a function of θ and ϕ:

$$\sigma(\theta, \phi) = A + B\cos 2\phi + C\sin 2\phi + D\cos\phi + E\sin\phi \quad \text{(B-5)}$$

where

$$A = \sigma_{iso} + [\tfrac{1}{6}\Delta\sigma(3\cos^2\chi - 1) + \tfrac{1}{4}\delta\sigma\sin^2\chi\cos 2\eta](3\cos^2\theta - 1)$$

$$B = [\tfrac{1}{2}\Delta\sigma\sin^2\chi + \tfrac{1}{4}\delta\sigma(\cos^2\chi + 1)\cos 2\eta]\sin^2\theta$$

$$C = -\tfrac{1}{2}\delta\sigma\cos\chi\sin 2\eta\sin^2\theta$$

$$D = (\tfrac{2}{3}\Delta\delta - \delta\sigma\cos 2\eta)\sin\chi\cos\chi\sin\theta\cos\theta$$

$$E = \delta\sigma\sin\chi\sin 2\eta\sin\theta\cos\theta \quad \text{(B-6)}$$

If the molecules are not completely aligned within the fiber

but have a distribution $P(\theta)$ of chain-axis orientations, we calculate the appropriate line shape from the integral

$$S(\omega) \propto \int_0^{2\pi} \int_0^{\pi} S_0[\omega, \sigma(\theta, \phi)]P(\theta)\, d\theta\, d\phi \quad \text{(B-7)}$$

where $S_0[\omega, \sigma]$ is the line shape of a single spin package with chemical shift σ. The position and width of this single line shape must be determined with the correct scaling factor and broadening dependence on the offset. For a completely aligned fiber sample, we have $P(\theta) = \delta(\theta - \theta_0)$, where θ_0 is the angle between the macroscopic fiber direction and the magnetic field; for a randomly oriented powder, $P(\theta) \propto \sin\theta$. We assumed that the molecules in our fibers had a Gaussian distribution with a standard deviation of Δ, which to a good approximation corresponds to

$$P(\theta) \propto \exp[-(\theta - \theta_0)^2/2\Delta^2] \sin\theta \quad \text{(B-8)}$$

In the computer simulation of the fiber REV-8 spectra taken at 108 °C, we took σ_{xx}, σ_{yy}, and σ_{zz} as well as the line broadening coefficients as fixed parameters (obtained from the powder spectrum) and determined the polar angles χ and η and the standard deviation Δ by least-squares curve fitting. A few of the fitted line shapes are shown in Figure B-2. The average results of the various fits are $\chi = 12 \pm 3°$, $\eta = 50 \pm 15°$, and $\Delta = 11 \pm 2°$. The least satisfactory fit was found for the $\theta_0 = 0$ orientation, presumably because the orientation distribution is not exactly Gaussian. Similar line-shape simulations for temperatures above 30 °C are also consistent with an angular standard deviation of about 11°. Obviously, χ and η cannot be determined from these line shapes since the rotation about the chain axis is fast at these temperatures.

Ultimately, one would like to determine the three Eulerian angles which relate the ^{19}F chemical shift tensor to the geometry of the CF_2 group. However, the randomization of the azimuthal angle ϕ in the fiber samples as well as in the molecular reorientation process prevent the experimental observation of the needed third angular parameter in addition to χ and η. Garroway et al.[7] have approached this problem by assuming that one component of σ lies along the CF bond. Since we need to know only the parameters χ and η for the analysis of the macromolecular dynamics, we did not attempt to further determine the details of the tensor orientation.

Appendix C. Powder Chemical Shift Spectra and Relaxation Times for Planar Rotational Diffusion

The calculation of chemical shift line shapes in the presence of rotation of molecules has been reviewed by Spiess.[40] In particular, the case of rotation about a fixed molecular axis (planar rotation) has been calculated by Alexander et al.[41] and experimentally demonstrated by Pines et al.[42] These authors restricted themselves to planar rotations about a direction which coincides with one of the principal axes of the chemical shift tensor. Recently, their treatment has been generalized by Campbell et al.[43] to anisotropic rotational diffusion about an axis of arbitrary direction. As shown in Appendix B, the rotation of the fluorine atoms in the crystalline regions of PTFE is not about a principal axis of the chemical shift tensor, and the general treatment has thus to be followed in our case. However, our method of calculation differed from that of the above-mentioned authors[41-43] in that we did not invoke an expansion into spherical harmonics or Wigner matrix elements.

Since we are dealing with purely planar rotations, we chose to represent the angular dependence of the chemical shift in the form of $\sigma(\theta, \phi)$ of eq B-5 and B-6, where the angles θ and ϕ refer to the geometrical arrangement depicted in Figure B-1. Rotational motion about the chain axis gives rise to mixing of the azimuthal angles ϕ but leaves the polar angles θ unchanged. The computational procedure that most closely reflects the physics of the model is, therefore, to calculate separate line shapes, $I'(\theta, \omega)$, for a range of values of θ and to determine the total line shape by integration

$$I(\omega) = \int_0^{\pi/2} I'(\theta, \omega) \sin\theta\, d\theta \quad \text{(C-1)}$$

For the calculation of $I'(\theta, \omega)$ we followed the general stochastic Liouville procedure of Freed et al.[43,44] For that purpose we expressed the random rotational motion in terms of a planar diffusional operator

$$\Gamma = D\partial^2/\partial\phi^2 \quad \text{(C-2)}$$

with eigenvalues $\gamma_m = -m^2D$ and eigenfunctions $G_m(\phi) = (2\pi)^{-1} \exp(im\phi)$ ($m = 0, \pm1, \pm2, \ldots$). The ϕ-dependent Hamiltonian

$$\mathcal{H}(\phi) = \hbar\omega_0[1 + \sigma(\theta, \phi)]I_z \quad \text{(C-3)}$$

is being written in terms of these eigenfunctions

$$\mathcal{H}(\phi) = \hbar\omega_0 I_z + \hbar \sum_{k=-2}^{2} A_k G_k(\phi) \quad \text{(C-4)}$$

where the coefficients A_k are complex combinations of the expressions $A, \ldots, E$ in eq B-6. According to the usual procedure,[41-45] this leads to the infinite set of linear equations ($m = 0, \pm1, \pm2, \ldots$)

$$[(\omega - \omega_0) - im^2D - i/T_2]X_m - (2\pi)^{-1/2} \sum_{k=-2}^{2} A_k X_{m-k} = \delta_{m,0} \quad \text{(C-5)}$$

where i/T_2 represents the intrinsic line width. The absorption spectrum is given by

$$I'(\theta, \omega) \propto \text{Im}\, X_0 \quad \text{(C-6)}$$

The infinite set of equations may be written in matrix notation as

$$\mathbf{BX} = \mathbf{U} \quad \text{(C-7)}$$

where $\mathbf{B}$ is a band-diagonal matrix.

We found it sufficient to truncate the equations at $|m| = [(|A_1| + 2|A_2|)/D]^{1/2} + 2$ and to calculate $I'(\theta, \omega)$ for 20 values of θ between 0 and $\pi/2$. The truncated set of eq C-7 was solved by Gaussian elimination.

The line shapes obtained by this calculation have to be modified to account for the effects that arise from the nature of the multiple-pulse experiment. The theoretical aspects of these modifications have been dealt with at length in a recent paper,[21] where it was shown that the scaled values of the chemical shift have to be taken for the calculation of the line shapes and that the apparent correlation times need not be corrected as long as they are longer than the time between the radio-frequency pulses. To verify this in our spectra, we note that our diffusional model involves two correlation times, $\tau_1 = 1/D$ and $\tau_2 = 1/4D$.[13] The highest diffusion rate in Figure 8 is $D = 2$ kHz $= 1.3 \times 10^4$ s^{-1}, corresponding to $\tau_2 = 20$ μs which is in fact longer than the pulse spacing of 3.6 μs. The formalism used for this line-shape calculation cannot account for a nonlinear scaling factor and an offset-dependent broadening (see Appendix A). Instead, these effects were accounted for after the completion of the stochastic Liouville calculation. The results of the line shapes that most closely agreed with the experimental spectra are shown in Figure 8.

The relaxation times T_{1xz}^{REV} and $T_{1\rho}$ of the crystalline fraction in the temperature region around 20 °C are governed by the same motional process. However, the dominant interaction for these relaxation times is the dipolar interaction. Again, for this relaxation mechanism we have the two correlation times $\tau_1 = 1/D$ and $\tau_2 = 1/4D$. Since the main contribution to the fluctuating dipolar interaction comes from the two ^{19}F nuclei within a CF_2 group whose internuclear vector is nearly perpendicular to the axis of rotation, it is τ_2 that dominates T_{1xz}^{REV} and $T_{1\rho}$. In other words, T_{1xz}^{REV} reaches a minimum when $\tau_2 = 0.6 \times 3.6\ \mu s$,[13] which corresponds to $D = 18$ kHz. Extrapolation of the data plotted in Figure 9 predicts that this would occur at 35 °C. Similarly, the $T_{1\rho}$ minimum is expected, where $2\omega_1\tau_2 = 1$ or $D = {}^1/_2\omega_1$. For a spin-lock field of 60 kHz this would be at 37 °C, where the diffusion rate is 30 kHz.

References and Notes

(1) Wilson, C. W.; Pake, G. E. *J. Chem. Phys.* **1957**, *27*, 115.
(2) Slichter, W. P. *J. Polym. Sci.* **1957**, *24*, 173.
(3) Hyndman, D.; Origlio, G. F. *J. Appl. Phys.* **1960**, *31*, 1849.
(4) McCall, D. W.; Douglass, D. C.; Falcone, D. R. *J. Phys. Chem.* **1967**, *71*, 998.
(5) McBrierty, V. J.; McCall, D. W.; Douglass, D. C.; Falcone, D. R. *Macromolecules* **1971**, *4*, 584.
(6) Ellett, D.; Haeberlen, U.; Waugh, J. S. *J. Polym. Sci., Polym. Lett. Ed.* **1969**, *7*, 71.
(7) Garroway, A. N.; Stalker, D. C.; Mansfield, P. *Polymer* **1975**, *16*, 171.
(8) Mehring, M.; Griffin, R. G.; Waugh, J. S. *J. Chem. Phys.* **1971**, *55*, 746. (a) Schaefer, J.; Stejskal, E. O.; Buchdahl, R. *Macromolecules* **1975**, *8*, 291. (b) *Ibid.* **1977**, *10*, 384.
(9) English, A. D.; Vega, A. J. *Macromolecules* **1979**, *12*, 353.
(10) Pembleton, R. G.; Wilson, R. C.; Gerstein, B. C. *J. Chem. Phys.* **1977**, *66*, 5133.
(11) Binsch, G. *J. Am. Chem. Soc.* **1969**, *91*, 1304.
(12) (a) Mehring, M. *NMR. 1976* **1976**, *11*. (b) Haeberlen, U. *Adv. Magn. Reson., Suppl. 1* **1976**.
(13) Vega, A. J.; Vaughan, R. W. *J. Chem. Phys.* **1978**, *68*, 1958.
(14) English, A. D.; Garza, O. T. *Macromolecules* **1979**, *12*, 351.
(15) Rhim, W.-K.; Elleman, D. D.; Vaughan, R. W. *J. Chem. Phys.* **1973**, *59*, 3740.
(16) Rhim, W.-K.; Elleman, D. D.; Schreiber, L. B.; Vaughan, R. W. *J. Chem. Phys.* **1974**, *60*, 4595.
(17) Eby, R. K.; Sinnott, K. M. *J. Appl. Phys.* **1961**, *32*, 1765.
(18) Sperati, C. A.; Starkweather, H. W. *Fortschr. Hochpolym. Forsch.* **1961**, *2*, 465.
(19) Ryland, A. L. *J. Chem. Educ.* **1958**, *35*, 80.
(20) McBrierty, V. J. *Polymer* **1974**, *15*, 503.
(21) Vega, A. J.; English, A. D. *J. Magn. Reson.* **1980**, *37*, 107.
(22) McCrum, N. G.; Read, B. E.; Williams, G. "Anelastic and Dielectric Effects in Polymeric Solids"; Wiley: New York, 1967. Also see ref 4.
(23) Starkweather, H. W., unpublished review.
(24) Bunn, C. W.; Howells, E. R. *Nature (London)* **1954**, *174*, 549.
(25) Spin–lattice relaxation times were measured and semiquantitatively agree with those reported in ref 4. There is no indication that the α relaxation is detectable with T_1 measurements.
(26) Diehl, P.; Khetrapol, C. L. *NMR. 1969* **1969**, *1*.
(27) Petersen, N. O.; Chan, S. I. *Biochemistry* **1977**, *16*, 2657.
(28) Bocian, D. F.; Chan, S. I. *Annu. Rev. Phys. Chem.* **1978**, *29*, 307.
(29) Bates, T. W.; Stockmayer, W. H. *Macromolecules* **1968**, *1*, 12, 17.
(30) Brown, R. G. *J. Chem. Phys.* **1964**, *40*, 2900.
(31) Martin, G. M.; Eby, R. K. *J. Res. Natl. Bur. Stand., Sect. A* **1968**, *72A*, 467.
(32) Clark, E. S. *J. Macromol. Sci.—Phys.* **1967**, *B1* (*4*), 795.
(33) Rabolt, J. F.; Piermarini, G.; Block, S. *J. Chem. Phys.* **1978**, *69*, 2872.
(34) (a) Rabolt, J. F.; Fanconi, B. *Polymer* **1977**, *18*, 1258. (b) Reneker, D. H.; Fanconi, B. *J. Appl. Phys.* **1975**, *46*, 4144.
(35) Reneker, D. H.; Fanconi, B. M.; Mazur, J. *J. Appl. Phys.* **1977**, *48*, 4032.
(36) Clark, E. S.; Muus, L. T. International Union of Crystallography, 6th International Congress, Rome, 1963; A-96. *Polym. Prepr., Am. Chem. Soc., Div. Polym. Chem.* **1964**, *5*, 17.
(37) de Gennes, P. G. *J. Chem. Phys.* **1971**, *55*, 572.
(38) Hentshel, D.; Sillescu, H.; Spiess, H. W. *Makromol. Chem.* **1979**, *180*, 241.
(39) McBrierty, V. J.; McCall, D. W.; Douglass, D. C.; Falcone, D. R. *J. Chem. Phys.* **1970**, *52*, 512.
(40) Spiess, H. W. *NMR. 1978* **1978**, *15*.
(41) Baram, A.; Luz, Z.; Alexander, S. *J. Chem. Phys.* **1976**, *64*, 4321.
(42) Reference 12a, p 39.
(43) Campbell, R. F.; Meirovitch, E.; Freed, J. H. *J. Phys. Chem.* **1979**, *83*, 525.
(44) Freed, J. H.; Bruno, G. V.; Polnaszek, C. F. *J. Phys. Chem.* **1971**, *75*, 3385.
(45) Vega, A. J.; Fiat, D. *J. Magn. Reson.* **1974**, *13*, 260.

Time-Resolved Fluorescence Emission Spectroscopy of Poly(phenylacetylene)

J. R. MacCallum,[1a] C. E. Hoyle,[1b] and J. E. Guillet*

Department of Chemistry, University of Toronto, Toronto, Canada M5S 1A1.
Received April 16, 1979

ABSTRACT: The fluorescence characteristics of a sample of poly(phenylacetylene) are reported for solutions in fluid and solid matrices. It is proposed that two emitting states are responsible for the fluorescence, and variation with solvent depends more on the polarizability of the solvent than on its physical state.

The photophysical behavior of polyenes has been the subject of much discussion, and anomalies still exist between theoretical predictions and experimental observations.[2-6] Recently, evidence has been presented illustrating corresponding trends among polymeric materials incorporating polyene structures.[7-11] Some of the unusual spectroscopic properties of polyenes can be rationalized by postulating the existence of two excited singlet states, one with B_u symmetry and the other with A_g symmetry. Transitions from the $^1A_g{}^0$ ground state are allowed to the $^1B_u{}^*$ state, but dipole forbidden to the $^1A_g{}^*$ state. These two excited states are separated by a small energy gap which varies with solvent polarizability.[6]

There is a notable distinction between the characteristics of polymeric systems which incorporate polyenes and those of small molecules, in that the polymeric chromophores apparently exhibit emission from two states.[10,11] For example, it has been shown that the fluorescence emission spectrum of a styrene/phenylacetylene copolymer comprises two bands, one centered at 420 nm and the other at 490 nm.[11] The higher energy component has a shorter lifetime than that at lower energy. Two possible mecha-

0024-9297/80/2213-1647$01.00/0